

MODELLING AND SIMULATION OF A SEASONAL UNDERGROUND WATER STORAGE COUPLED WITH PHOTOVOLTAIC PANELS, HEAT PUMP AND DISTRICT HEATING NETWORK FOR PROVIDING LOCAL RENEWABLE HEATING TO A RESIDENTIAL DISTRICT

Aitor Cendoya^{1*}, Frederic Ransy^{1,2}, Vincent Lemort¹, Natalia Kozłowska¹, Pierre Dewallef¹, Jacques Windeshausen²

¹Thermodynamics Laboratory, Faculty of Applied Sciences, University of Liège, Belgium

²Wingest Energy, Bastogne, Belgium

*Corresponding Author: acendoya@uliege.be

ABSTRACT

Energy storage is a key component to face the intermittence of renewable energy and achieve decarbonization of the electricity grid by 2050. In this regard, this paper assesses the potential of seasonal energy storage in flooded underground mines. The analysis is based on a case study of a slate mine in Martelange, southern Belgium. The models presented assess the heating and cooling energy demands of a complex of 50 apartments. The study site comprises a photovoltaic plant, which supplies a water-to-water Heat Pump (HP), that is used to heat an underground cavern of 6840 m³ flooded with water, while an adjacent cavern of 80000 m³ is used as a cold reservoir. The hot cavern is charging during the summer period, reaching a maximum temperature of 55°C, and discharging in winter until 40 °C. The District Heating Network (DHN) is modelled to transport the hot water to each apartment where a buffer tank is used to reheat the water by a secondary HP for Domestic Heat Water. The system has been modelled in Dymola and simulated for 4 years with a step time of 15 minutes. The study case can cover 76.7% of the total building heating demand throughout the DHN, within a COP of 2.86. These results underline the potential of reusing mine caverns for robust energy storage solutions, promoting a shift towards renewables and establishing opportunities for interconnected multi-system grids.

1 INTRODUCTION

The global climate has undergone noticeable degradation in recent years, despite concerted efforts by various international organisations to achieve energy grid decarbonization by 2050 (Energy Agency, 2021). For this, important agreements, such as the Kyoto Protocol and the Paris Agreement, have been established to limit the increase in global temperature to 1.5°C (Wei et al., 2022). To achieve these goals, it is imperative to increase the proportion of Renewable Energy Sources (RES) in the energy mix and effectively manage the energy supply (Vecchi et al., 2022). Nevertheless, RES inherently exhibit fluctuations and instability, potentially resulting in mismatches between producers and consumers. Thus, energy storage emerges as a pivotal element in the energy transition, serving as a bridge between producers and users (Olympios et al., 2020).

The energy storage technologies have been classified into four main groups: mechanical, electromechanical, chemical and thermal energy storage (Olabi et al., 2021). Among these, Thermal Energy Storage (TES) promises to be the most suitable for large energy storage applications due to its environmental friendliness and comparatively low capital costs (Luo et al., 2015). Today, attention has increased towards Seasonal Thermal Energy Storage (STES) systems, as they can store surplus solar energy from RES during summer to compensate for low production during the winter (Bott et al., 2019). These storage systems can be integrated into District Heating Networks (DHN) to fulfil the heating requirements of residential complexes. This contributes to reducing CO₂ emissions, given that the building sector represents the third-largest consumer of primary energy (Cabeza et al., 2022).

Abandoned underground mines represent systems with substantial energy storage capacity. Therefore, it is essential to investigate the applications of such storage in the energy transition. This paper evaluates the feasibility of reusing a flooded abandoned slate mine, in the city of Martelange, Belgium, as a Seasonal Underground Thermal Energy Storage (SUTES) system. The objective is to demonstrate the integration of renewable energy sources in an abandoned space flooded with water to provide heating and cooling within a neighbourhood, to partially decouple the system from the electricity grid or fossil fuels. For that, the water inside one of the caverns will be heated by a Heat Pump (HP). Once the system has reached the required thermal inertia after two years, it is expected to be able to cover a large part of the heating demand of a 50-apartment complex through a DHN.

2 METHODOLOGY

The following section describes the methodology employed to assess the case study. Describing first the climatic conditions used to evaluate the whole system for afterwards describing the model employed in Dymola software (Dempsey, 2006) tool to represent the real system behaviour.

2.1 Climatic Conditions

The climatic conditions are extracted from EnergyPlus (Crawley et al., 2001) and correspond to a typical year (average conditions at the same location based on the last 20 years of historical data) starting from the 1st of January to the 31st of December. These conditions are extracted in intervals of 1 hour. Figure 1 illustrates the monthly averages of dry bulb temperature (T_{amb}), relative humidity and the global horizontal radiation. The atmospheric pressure remains almost constant to 0.94 atm. This typical year is considered for the numerical simulation over the 4 years.

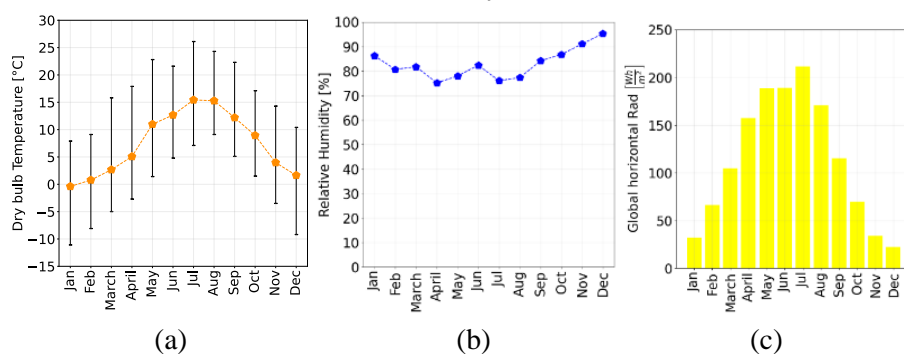


Figure 1: Monthly average of a) T_{amb} , b) relative humidity and c) global horizontal radiation

2.2 Component Models

This section presents the dynamic models encompassing the whole system to analyse and assess the case study configuration. Each component is meticulously modelled in a modular approach, facilitating their subsequent integration into an overall system.

2.2.1 Buildings

The residential complex of buildings to be modelled corresponds to 5 buildings regarding a total number of 50 apartments. Each building shares an identical structure, with a distribution across two floors: four apartments per floor and an additional two on the top floor. Figure 2 provides a visual representation of the building's location in Martelange, and the respective zone for floors 1-2.

Given the substantial computational resources required to simulate the heating and cooling demand of the residential complex, the following assumptions are considered. Firstly, the total heating and cooling demand estimation is performed for a single building and then multiplied by a factor of 5 to have the global values. Secondly, within the Dymola model, the emphasis is placed on the apartment most significantly affected by its orientation. In both cases, the heating and cooling demand is multiplied by a factor of 50 representing the total number of flats. This generates an error of 6% and allows for the

representation of the physical and dynamic behaviour of the residential building complex, reducing the simulation time without compromising the real behaviour of the whole system.



Figure 2: Building assessed a) location in Belgium, b) zone discretization for the 1st and 2nd floors

Table 1 presents the area and volume of each zone considered. Noted all zones have the same height and correspond to 3 m. The layout of these zones adheres to square geometry exclusively within the apartments. The total area covered by the apartments amounts to 8906 m².

Table 1: Geometry and distribution of the zones discretized.

Floor	Zones	Rooms	A [m ²]	V [m ³]
First and Second Floor	Z ₁	Living room	41.7	125.0
	Z ₂	Bedroom 2	9.6	28.7
	Z ₃	Hall, Laundry room and W/C	8.5	25.6
	Z ₄	Bathroom and Night-Hall	8.6	25.9
	Z ₅	Bedroom 1	14.5	43.5
Third Floor	Z ₁	Living room and Pantry	53.2	159.5
	Z ₂	Bedroom 1	16.8	50.4
	Z ₃	Bathroom and Night-Hall	10.9	32.7
	Z ₄	W/C and Night-Hall	7.5	22.4
	Z ₅	Bedroom 2	11.6	34.9
	Z ₆	Bedroom 3	13.7	41.1

The occupant schedules for the rooms are based on the standard ISO 17772-1. Furthermore, the occupants within the zone are assumed to engage in office work activity. To evaluate thermal comfort within the zone, the thermal comfort model of Fanger is employed. Thus, parameters and information are integrated into the Zone blocks available in the IDEAS library, which considers the heat transfer between the different layers of the materials, internal walls, opaque walls and windows, as well as longwave and shortwave radiation. For more comprehensive insights and detailed equations of the model, refer to the study by Jorissen et al. (2018).

2.2.2 Radiant Slab

The heating delivery to the buildings is provided by a radiant slab system positioned on the floor of each apartment. Specifically, this heat source is installed in Zones 1, 2, 4, and 5 for the apartments located on the 1st and 2nd floors. For the apartments on the 3rd floor, the zones correspond to 1, 2, 3, 5 and 6. Other zones are excluded from heating considerations as they represent areas where occupants spend only a few minutes of the day. The heat flow rate for the radiant slab is calculated based on a surface heat flow value of 40 W m⁻². Moreover, a pressure drop of 30 kPa along the cycle is taken into account, and the radiant floor is positioned at half of the floor depth.

The radiant slab model considers several parameters which are based on EN 15377-1 and the work developed by Koschenz et al. (2000) for Thermally Active Building System (TABS). The block employed for the model of the radiant slab corresponds to the RadinatSlab.EmbeddedPipe available in

the IDEAS library. The radiant slabs employ a control strategy aimed at maintaining the set-point temperature within each zone. This control is implemented using hysteresis, which compares the zone temperature with three set points. During heating mode, the set point is 20°C between 7 a.m. and 24 p.m., and 18°C between 24 p.m. and 7 a.m. For cooling mode, the set point is maintained at 27°C throughout the day. Additionally, a control system is integrated at the supply of the radiant slab. This control system utilizes a PI control, aiming to adjust the temperature to 35°C by controlling a three-way valve, which controls the percentages of water streams. For cooling, the groundwater is directly supplied to the radiant slab circuits, where the setpoint temperature for the cooling mode is 12°C.

2.2.3 Apartment Buffer Tank

Each apartment is equipped with a tank at the building level, responsible for distributing hot water for both Space Heating (SH) and Domestic Hot Water (DHW). The tank comprises three heat exchangers (HE): one for the heat transfer from the DHN, the condenser of the HP, and the third one which raises the temperature of the radiant slab circuit. This configuration ensures an efficient and controlled supply of hot water for both SH and DHW in each apartment.

The volume of the tank corresponds to 300L of which 200L are dedicated to DHW. The supply temperature of this water corresponds to the usual temperature of the tap water (12°C). The nominal heat power of the HE corresponds to 6 kW, 9 kW and 3 kW for the DHN, SH and HP, respectively. This model is based on a modification of the StratifiedEnhancedInternalHex block available in the IDEAS library. This block discretises the entire volume into 10 sub-volumes that interact with upstream and downstream ones, transferring mass and energy. The height of the tank corresponds to 215 cm, where the DHN HE is connected from the bottom to a height of 60 cm, followed by the SH HE from 20 cm to 160 cm, and finally the HP HE from 140 cm to 200 cm. This distribution allows for adequate control of the temperature stratification in the tank to cover the required heat quantities at different temperatures.

The control system of the tank is a stratified control system aiming for three different temperature set points. The first set point corresponds to the HP located at the top of the tank, which employs an ON/OFF control mechanism. The second set point controls the electrical resistance, also utilizing an ON/OFF control and is positioned in the middle of the tank. The third set point corresponds to the DHN connection, where heat is extracted from the network if the temperature at the bottom of the tank is lower than the specified values. This control system operates to maintain temperatures between 50-55°C at the top and between 40-45°C at the bottom of the tank, ensuring efficient heating for SH and DHW within each apartment.

2.2.4 Photovoltaics Panel (PV)

The PV block is built to represent the electricity production which can be reached at the study site. The idea of the PV installation is to have a free energy source to feed the main HP. The available area in the study site corresponds to 388 m², which will be covered with PV panel HIP 230HDE1 from Sanyo manufacturer. These panels are inclined at an angle of 30° to optimize solar energy capture efficiency. The model of the PV panel corresponds to the five-parameter model presented by Duffie and Beckman (1991), which is based on the single-diode equivalent circuit of a PV panel. The parameters correspond to the thermal voltage, the series resistance, the shunt resistance, the diode reverse saturation current and the light current. The calibration of the 5-parameter model is based on the limited information provided by manufacturers. The block employed corresponds to the PVSystemGeneral available in the experimental section of the IDEAS library.

2.2.5 Electrical Battery (EB)

The EB model is concerned according to the model proposed by Modelica Standard Library. This model considers that there exists a direct dependence between the State Of Charge (SOC) and the Open Circuit Voltage (OCV), thus meaning while more charge the battery it will be higher the voltage. As well when the battery is fully charged, it starts to self-discharge through a nominal current, which depends on the current provided by the manufacturer. The influence of cell temperature on battery behaviour is not

accounted for in this model, as experimental parameters are required to incorporate this aspect accurately corresponding to 550 Ah, which is achieved by a square arrangement of 55 cells. Each one corresponds to a capacity of 10 Ah with an OCV maximum of 4.2 V and a minimum of 2.5 V.

2.2.6 Heat Pump (HP)

The HP serves as the central component of the underground storage system, responsible for converting electrical energy into heat. Various options are available for modelling that device in Dymola, and the most suitable one is chosen from the existing blocks in the IDEAS library. In this case, the water-to-water model is employed to represent both, the main HP, and the back-up HP. The parameters of the systems are selected based on the Viessmann manufacturer, specifically the model Vitocal 300G BW 301.A29, with a nominal heat capacity of 140 kW (\dot{Q}_{cd}) for the main HP, and 60 kW for the back-up HP. The dynamic modelling approach is derived from the PhD thesis of Jin (2002). In the case of heat exchangers, the epsilon-NTU model is considered, which relates the UA (model parameter) to the capacitive flow rate, which varies with time. For the compressor, the power is calculated from the theoretical consumption and the dynamic effect is represented in the calculated variables, such as compressor speed and feed conditions. Further reviews and verifications of the implementation and validation of this model can be found in Filonenko et al. (2020) and Jorissen et al. (2018).

The main HP operates within a battery SOC range of 99% to 10%. However, once the SOC level drops to 10%, the HP will deactivate until the SOC level reaches 50%. This ensures that the HP can operate for at least 1.5 hours until the battery is recharged. The backup HP is activated under two conditions: firstly, when the ambient temperature falls below 5°C, and secondly, when the SUTES temperature drops below 40°C after two years of operation. This energy source is sourced from the grid and is utilized to maintain a balance in the SUTES. Additionally, both HPs will stop if the temperature supply to the condenser exceeds 60°C due to limitations imposed by the working fluid (R410A) pressures.

2.2.7 Underground Reservoir

In the past, the study site functioned as a slate mine, with mining operations ongoing until 1990 when they ceased. Today, the abandoned mine is flooded with water, as shown in Figure 3. The primary objective is to evaluate the feasibility of utilizing the underground cavern for energy storage purposes.



Figure 3: Study site a) passages connection between caverns, b) caverns to be used as an energy reservoir, c) 3-D view of the whole mine

The abandoned mine considers 9 interconnected caverns, with the highest depth of 180 decreasing from east to west. For this paper, 2 of the 9 chambers will be employed as energy reservoirs, one for the cold reservoir (80000 m³ at 10°C) and one for the hot reservoir (6840 m³ at 40-50°C). The reservoir sizes are the actual and available volumes in the different caverns. The thermodynamic properties of the slate λ_{soil} , ρ_{soil} and $c_{p,\text{soil}}$ corresponds to 2.57 W m⁻¹K⁻¹, 2750 kg m⁻³ and 837 J kg⁻¹K⁻¹, respectively. The initial temperature of the soil and water is considered 10°C (Grabenweger et al., 2021).

The underground model is constructed using multiple mixed volumes (10), which serve to approximate the discretization within the underground storage. These volumes function as mixing volumes, effectively blending all incoming fluids without pressure drop into the volume and with a uniform

temperature (Wetter & Van Treeck, 2017). To represent heat losses from the caverns and the underground storage, thermal resistance ($R_{\text{soil}} = \ln((D_{\text{UND}}/2 + x_{\text{soil}})/(D/2)) / (2 \cdot \pi \cdot x_{\text{soil}} \cdot \lambda_{\text{soil}})$) and capacitance ($C_{\text{soil}} = ((\pi \cdot (D + x_{\text{soil}})^2/4 - A_{\text{UND}} \cdot h_{\text{UND}}) / (\rho_{\text{soil}} \cdot c_{p,\text{soil}}))$) of the slate are incorporated into the model, here x_{soil} corresponds to the distance where the soil temperature is calculated and corresponds to a radial distance of 10 m. These variables are directly connected to the volumes to calculate the heat transfer between water and soil due to the temperature difference. The model defines the time-dependent state for mass and energy balance within the volumes. The model assumes that the volumes have a constant density and mass fraction.

The cold reservoir is regenerated through the soil, both start at the same temperature during the simulation and, as the water temperature decreases, the soil releases heat. By the end of the 4th year, the soil reaches a temperature of 6°C, partially regenerating the reservoir. Therefore, it is essential to find a process in which water can be regenerated. One of the possible uses for the water is to supply cooling water through a DHN. This makes the system capable of providing a large amount of cold to companies that need cooling. If the water temperature is not low enough, it could be further decreased by a chiller. However, in case it is not possible to find interested stakeholders, it is necessary to circulate water from the medium-temperature reservoir to regenerate the cold reservoir and maintain operational safety.

2.2.8 District Heating Network

DHN functions as the distribution network between the underground storage and the end-users. Given its critical role, a detailed model representing the physical principles is imperative. This model assumes direct contact between the pipes-insulation and the surrounding soil, necessitating the consideration of a fixed temperature of 10°C to represent the soil. For this purpose, the PlugFlow model available in the International Building Performance Simulation Association (IBPSA) library is employed. The validation of this model has been extensively detailed in the work of Wetter and Van Treeck (2017). This model allows for the effect of heat losses to be represented as well as the pressure drop in the DHN from the underground reservoir, which is 50 m below ground level, to the return of the DHN to the caverns, with a total length of 324 m.

2.3 Overall Connection

The overall connections of the components are imposed according to the scheme presented in Figure 4. The electrical energy flows from the PV electricity production going to the electrical cabin where is the battery module which feeds with electricity the main HP which is employed for heating-up and cooling-down the underground storages. Then this thermal energy is stored to be transported by the DHN until the apartment's levels for the supply part of the SH and DHW.

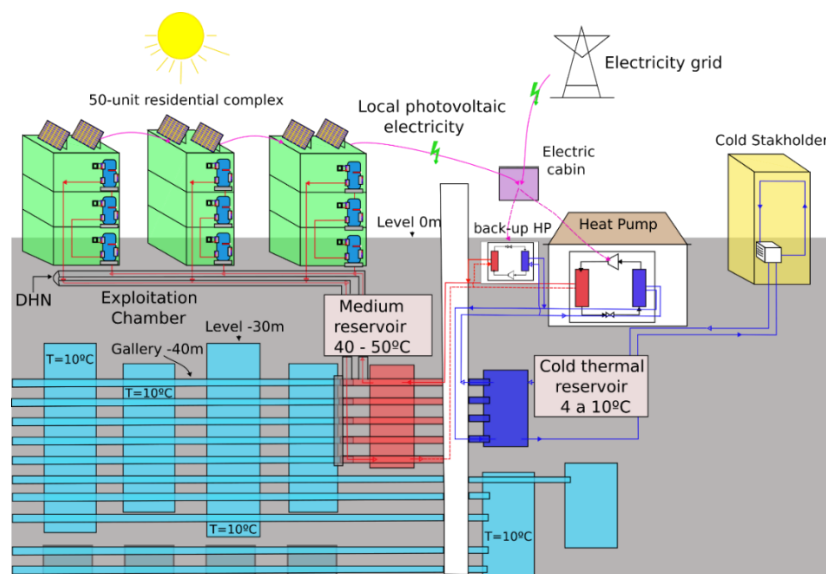


Figure 4: Scheme of the overall connection of the study case in Martelange, Belgium

Several global assumptions are made in the simulation:

1. The system operates for two years, during which all energy is stored without any utilization.
2. The charging of the reservoir during the first two years is done by the main HP. After this period, the back-up HP is available to assist the heating process.
3. The simulation considers a single apartment, where the heating and cooling demand is scaled by a factor of 50. This assumption introduces an error of approximately 1.2% per building, which can lead to a total error of 6%. However, it reduces the simulation time considerably.

To evaluate the global performance of the system different coefficients are considered. The first corresponds to SUTES heat losses which is presented in Eq. 1. The second corresponds to the energy storage efficiency presented in Eq. 2, which compares the discharged energy against the charged energy. The third one, Eq. 3 corresponds to the efficiency of energy transfer to the water in the SUTES, which corresponds to the net energy value of the stored energy divided by the total energy supplied. Finally, the global COP of the system also is computed through Eq. 4 which compares the whole electrical inputs and the heating supply to the end-users.

$$E_{UND,loss} = \sum_{i=1}^{i=10} \int_{t_{in}}^{t_f} \frac{T_{w,vol,i}(t) - T_{soil,i}(t)}{R_{soil,i}} dt \quad (1)$$

$$\eta_{sto} = \frac{\int_{t_{in}}^{t_f} \dot{M}_{w,DHN} \cdot c_{p,w} \cdot (T_{w,su,DHN} - T_{w,ex,DHN}) dt}{\sum \int_{t_{in}}^{t_f} \dot{M}_{w,HP,j} \cdot c_{p,w} \cdot (T_{w,ex,HP,j} - T_{w,su,HP,j}) dt} \quad (2)$$

$$\bar{E}_{sto} = \frac{\sum \int_{t_{in}}^{t_f} \dot{M}_{w,HP,j} \cdot c_{p,w} \cdot (T_{w,ex,HP,j} - T_{w,su,HP,j}) dt - E_{UND,loss}}{\sum \int_{t_{in}}^{t_f} \dot{M}_{w,HP,j} \cdot c_{p,w} \cdot (T_{w,ex,HP,j} - T_{w,su,HP,j}) dt} \quad (3)$$

$$COP_{sys} = \frac{\int_{t_{in}}^{t_f} \dot{Q}_{build}(t) + \dot{Q}_{DHW}(t) dt}{\int_{t_{in}}^{t_f} \sum \dot{W}_{aux}(t) + \sum \dot{W}_{cp,HP,j}(t) + \sum \dot{W}_{tk,app}(t)} \quad (4)$$

3 RESULTS AND DISCUSSION

The system was simulated for 4 years with a time step of 15 minutes in the Dymola software. The total number of equations solved corresponds to 26716, being a system of algebraic-differential equations, which is solved by the Dassl method. The main idea of this system is to contribute to decarbonisation and facilitate multi-system integration. First of all, it is essential to describe the heat demand that must be covered by the system. This value was calculated for one building and multiplied by 5, resulting in a total annual heat demand of 387.2 MWh/y for SH, and 182.5 MWh/y for DHW. Therefore, the total energy required to meet the demand of all 50 apartments amounts to 569.7 MWh/y.

The study case aims to supply the energy heating demand of 50 apartments through SUTES. Initially, the SUTES is heated by the main HP using energy from a PV array. After two years, the backup HP works together with the main HP. For this purpose, the energy transfer from the PV array corresponds to 88.1 MWh/y with a peak of 77.1 kW. This energy is transferred to the electric battery which works as a buffer to supply the HP main compressor. The average PV self-consumption of the system after two years of charging the SUSTES corresponds to 95.2%. On the other hand, the backup HP takes energy from the grid to support the underground reservoir during the winter period when the heating demand is higher.

The efficiency of energy transfer to the water in the SUTES (\bar{E}_{sto}) is low in the first two years, reaching a value of 43% and 30.6%, respectively. This value decreases in the second year due to higher underground water temperatures, decreasing the heating capacity of the main HP. Heat losses are quantified as 269 and 248.2 MWh/y during the initial charging period, 1st and 2nd year, respectively. However, as the system begins operation, heat losses decrease significantly, reaching 70 and 44.3

MWh/y in the 3rd and 4th years, respectively. This reduction is attributed to the behaviour of the SUTES, which leads to oscillations in underground temperature. As a result, the soil releases heat to the SUTES, amounting to 7.5 MWh/y in the 3rd year and 30 MWh/y in the 4th year. Consequently, (\bar{E}_{sto}) increases to 87% and then 92% indicating improved energy conservation efficiency over time.

The average energy transfer from the main HP corresponds to 318.9 MWh/y and 234 MWh/y for the backup HP. These energy transfers exhibit an opposite trend; the main HP provides more energy to SUTES during the summer months, facilitated by the large amount of energy generated by the PV panels. In contrast, the backup HP transfers energy during winter when the T_{amb} is low and the heating demand is high. Figure 5 presents the SUTES heat losses to the soil during the system operation (3rd and 4th years). It is evident that in the 3rd year, the heat losses are higher compared to the 4th year, primarily due to the starting conditions of 50°C compared to 40°C, respectively. Additionally, the seasonal behaviour of SUTES is evident being charged during the summer for discharge during the winter months. Furthermore, the η_{sto} in terms of energy charged compared to the discharge indicates a recovery rate of 79% for the 3rd year and 78.6% in the 4th year. This highlights that 80% of the total energy charged in the SUTES can be recovered during the discharging process.

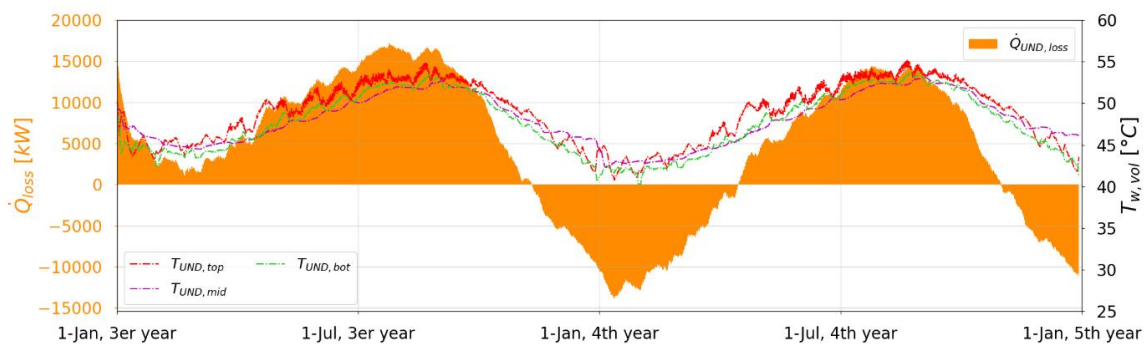


Figure 5: SUSTES temperature and heat losses during the 3rd and 4th years

These temperatures presented correspond to the calculated value at the top, middle and bottom of the discretised hot reservoir. The upper part corresponds to the volume where the hot water is discharged from the HP, and the lower part corresponds to the volume where the water is extracted and returned to the HP. This temperature variation affects the HP COP, making the performance less efficient during the summer when the lift temperature is higher.

The DHN extracts energy from the SUTES to transport heat to the apartment tanks. In the 3rd and 4th years of operation, the energy transferred corresponds to 442 and 430 MWh/y, respectively. This value is slightly higher in the 3rd year as the apartments do not have a high thermal inertia due to the non-heating of the zones during the 1st and 2nd years. This value corresponds to 76.8% and 76.5% of the whole heat demand of the buildings. The remaining heating demand (133.8 and 132.7 MWh/y) is covered by the HP and electrical resistance in the apartment tanks. This additional energy is drawn from the electricity grid, reaching 44.5 and 44.1 MWh/y. The PV self-production of the system corresponds to 44.5% for the 3rd and 4th years. Furthermore, through the PV-battery system, the surplus energy that is not stored in the battery due to being fully charged corresponds to 3.7 MWh/y, which can be used in the same installation to cover part of the auxiliary demand.

Figure 6 presents a typical day of operation during winter, showcasing how the heating demand of the building is covered. A significant portion of the heating demand is supplied by the DHN, which transports heat from the SUTES. Performing a role in regulating the temperature in the apartment tank, activating when the temperature in the bottom part falls below 40°C. On the other hand, due to low PV production during this period, the main HP is activated for nearly 2 h of the day. However, the back-up HP ($\dot{W}_{cp,HP,bk}$) operate a large portion of the day, which is related to the winter season when temperatures are lower.

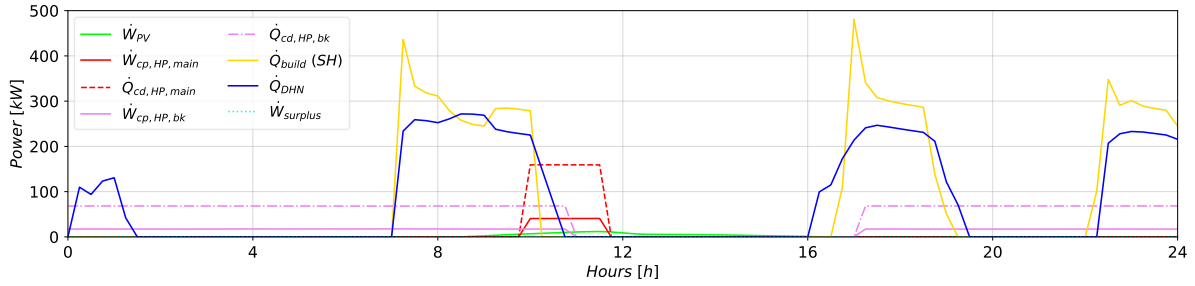


Figure 6: Working system during a winter typical day

Figure 7 presents a typical day of operation during summer, showcasing the opposite behaviour compared to winter. During this period, the system is primarily in charging mode due to the large amount of PV production. As a result, the main HP can operate for an extended duration, approximately 11.5 hours. Additionally, DHN is responsible for supplying a portion of heat for the DHW needs of the buildings, as the heating demand is negligible during summer. This graphic exemplifies that during summer when there is high PV production, the main HP operates for an extended period, while the back-up HP remains inactive (OFF) during this period.

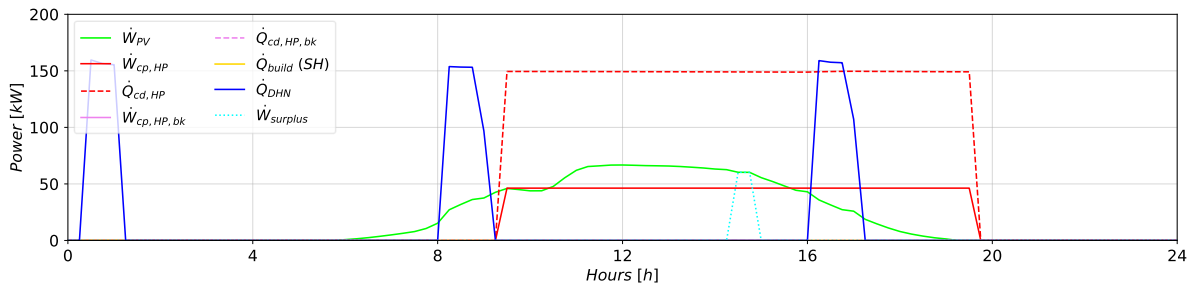


Figure 7: Working system during a summer typical day

The overall COP of the system computed according to Eq. 4 for the 3rd and 4th years corresponds to the ratio of the total heat supply for the system regarding the SH and DHW to the whole amount of energy required consumed. This amount is distributed by the main HP, the backup HP, the apartment HP, the electrical resistance, and the auxiliary components. This value for the 3rd year corresponds to a global COP of 2.86 and for the 4th year 2.81. These values reflect a successful operation of the system, where almost half of the electricity comes from RES.

To check if the system is satisfying the heating demand correctly, Figure 8 presents the temperature of one apartment for the different zones against the T_{amb} where it is possible to appreciate the efficient control for the radiant slab which can maintain the zones heated during the whole year. On the other side, the cooling demand of the buildings is 0 and this is due to the fact that with the selected weather file, the zone temperatures never reach a value higher than 27°C, which results in the cooling mode not being activated. This leads to a large volume of water (80000 m³) at 4°C which can be able to supply 465 MWh/y of cold for the stakeholders.

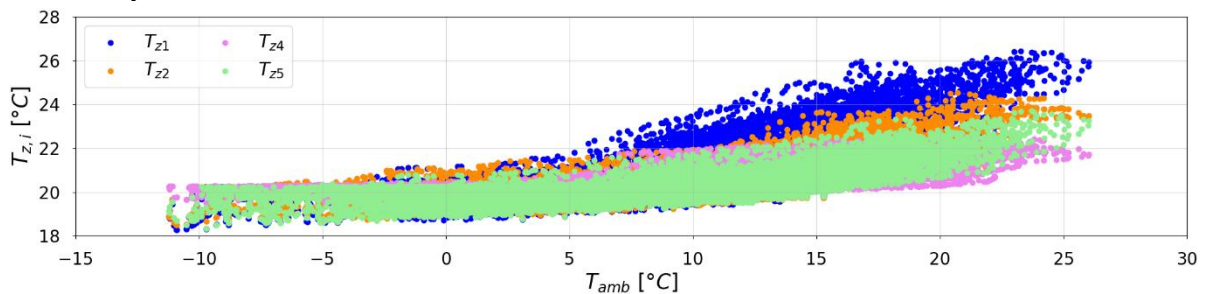


Figure 8: Zones temperature for different ambient temperatures

A summary of the main energy indicators for the 4 years of operation is depicted in Table 4. Values such as the positive heat losses ($E_{UND,loss}(+)$) as well as the negative heat losses recovered from the soil ($E_{UND,loss}(-)$) are presented. In addition, the thermal energy transfer by the main Hp ($E_{cd,HP,main}$) and the bk-up ($E_{cd,HP,bk}$) with their respective energy consumption ($E_{cp,HP,main}$, $E_{cp,HP,bk}$) are presented. The total heat demand of the buildings ($E_{heating}$), the energy production from the photovoltaic production and finally the corresponding variables from Eq.2 to Eq.4.

Table 4. Main variables from the simulation.

Years	$E_{UND,loss}(+)$ [MWh/y]	$E_{UND,loss}(-)$ [MWh/y]	$E_{cd,HP,main}$ [MWh/y]	$E_{cd,HP,bk}$ [MWh/y]	$E_{heating}$ [MWh/y]	$E_{cp,HP,main}$ [MWh/y]	$E_{cp,HP,bk}$ [MWh/y]	E_{PV} [MWh/y]	η_{sto}	\bar{E}_{sto}	COP_{sys}
1	269.0	0	471.7	0	182.5	72.2	0	88.1	-	0.43	-
2	248.2	0	357.6	0	182.5	82.3	0	88.3	-	0.31	-
3	70.0	7.5	322.5	236.8	575.8	84.5	53.9	88.1	0.79	0.87	2.86
4	44.3	30	315.3	231.8	562.7	84.4	53.0	88.2	0.78	0.92	2.81

In addition, the CO₂ emissions are compared with conventional systems such as gas boilers, biomass, and the electricity grid, providing insight into the imperative of employing this system to reduce CO₂ emissions and achieve independence from the grid. The emissions for the different sources have been quantified as: 426.5 kg CO₂/MW_{th}h, 93.4 kg CO₂/MW_{th}h and 100.7 kg CO₂/MW_eh, for gas boiler, biomass (Kazulis et al., 2018) and the Belgium electricity grid. Consequently, the CO₂ emissions of these systems amount to 243 tons CO₂/y for gas boilers, 53.1 tons CO₂/y for biomass, and 20.1 tons CO₂/y for the Belgian electricity grid. For the study case, this value corresponds to 11.4 tons CO₂/y, which potential can reach zero if the PV area is increased and the chamber volume is expanded. This highlights the system's potential for significant reductions in CO₂ emissions

4 CONCLUSIONS

To increase the penetration of renewable energies in the electrical grid, employing energy storage methods is indispensable to achieve the decarbonization of the energy grid by the year 2050. Therefore, this article presents an innovative large-scale SUTES solution, specifically a flooded abandoned mine in the city of Martelange, Belgium. The approach not only underscores the importance of repurposing existing infrastructures for sustainable energy solutions but also highlights the potential of SUTES. The proposed system uses a large quantity of RES to generate heat and store it in a cavern, achieving a PV self-consumption of 95% with a 388 m² area. After two years of supplying energy to the SUTES to gain thermal inertia, the volume of 6840 m³ provides energy to a DHN system capable of covering 76.65% of the heat demand for SH and DHW for a residential complex of 50 apartments.

The energy conservation in the SUTES during the 1st and 2nd years is affected significantly by the heat losses. However, by the 3rd year, when the whole system starts operating, the storage system achieves an energy conservation of 89% and is able to recover 30 MWh/y from the ground, which is released during the discharge process. Additionally, the average overall COP of the system corresponds to 2.83, where almost half of the energy comes from renewable sources (81.4 MWh/y) and could be considered free. In addition to covering a significant portion of the heat demand through renewable energies, the system also significantly reduces CO₂ emissions, reducing a total of 231.6 tons of CO₂ compared to a gas boiler, 41.7 tons of CO₂ compared to biomass, and reducing emissions by 43.3% compared to extracting electricity from the grid. This paper highlights the potential of repurposing abandoned mines as energy storage systems, contributing to an efficient transition towards renewable energy sources.

This approach opens up new opportunities for establishing large-scale energy distribution networks in areas that have had environmental impacts and are no longer operational. Therefore, it would not only contribute to reducing CO₂ emissions but also serve revitalising areas that currently lack purpose. The system presents several operational challenges to maintain the safety of the equipment. The most relevant technical aspect is the chemical concentration of the water, so the reservoirs cannot be directly connected to the above-ground components. The estimated cost for the purchase and installation of the HPs is between 600-800 €kW_{th}⁻¹ and for the underground reservoirs it is 70 k€ (6000 m³). The advantage is that the reservoirs are part of the ground, so there is no need to pay for them or to build them from

scratch. This scenario is widespread in different abandoned mining sites in Belgium, which have been flooded by water over time.

The model limitation corresponds to:

- The assumption that was made to evaluate the entire apartment complex.
- The DHW was considered to be present only 3 times a day with a uniform demand.
- The consideration of the DHN running throughout the summer may lead to inefficient control.

Among the perspectives, the evaluation of the integration of the heat-power component to increase the flexibility of electricity production. The evaluation of weather files considering the heatwave or future scenario for the analysis of the system, however, in the next steps, these files will be integrated to analyse the performance of the selected components based on the typical year.

NOMENCLATURE

A	Area	(m ²)	cp	Compressor
C	Capacitance	(J/K)	DHN	District Heating Network
c_p	Specific Heat	(J/kg-K)	DWH	Domestic Hot Water
COP	Coefficient of Performance	(-)	ex	Exhaust
E	Energy	(MWh/y)	f	Final
\dot{M}	Mass Flow Rate	(kg/s)	HP	Heat Pump
\dot{Q}	Heat Flow Rate,	(kW)	in	Initial
R	Resistance	(K/W)	loss	Losses
t	Time	(h)	heat	Heating
T	Temperature	(°C)	main	main HP
V	Volume	(m ³)	PV	Photovoltaic panels
Z	Zone	(-)	rad	Radiant
\dot{W}	Energy Flow Rate	(kW)	slab	Slab
Greek letters			soil	Soil
η	Efficiency	(-)	sto	Storage
λ	Thermal conductivity	(W/m-K)	su	Supply
ρ	Density	(kg/m ³)	surplus	Surplus
Subscript			sys	System
Amb	ambient		tk	Tank
App	apartment		UND	Underground
Aux	auxiliary		vol	Volume
Build	buildings		w	Water
Bk	back-up		rec	Recovery
Cd	condenser			

REFERENCES

- Bott, C., Dressel, I., & Bayer, P. (2019). State-of-technology review of water-based closed seasonal thermal energy storage systems. In *Renewable and Sustainable Energy Reviews* (Vol. 113). Elsevier Ltd. <https://doi.org/10.1016/j.rser.2019.06.048>
- Cabeza, L. F., Q. Bai, P. Bertoldi, J.M. Kihila, A.F.P. Lucena, É. Mata, S. Mirasgedis, A. Novikova, & Y. Saheb. (2022). Buildings. In IPCC, 2022: Climate Change 2022: Mitigation of Climate Change. In *Contribution of Working Group III to the Sixth Assessment Report of the Intergovernmental Panel on Climate Change* (pp. 953–1048). Cambridge University Press. <https://doi.org/10.1017/9781009157926.011>
- Crawley, D. B., Lawrie, L. K., Winkelmann, F. C., Buhl, W. F., Huang, Y. J., Pedersen, C. O., Strand, R. K., Liesen, R. J., Fisher, D. E., Witte, M. J., & Glazer, J. (2001). EnergyPlus: creating a new-

- generation building energy simulation program. *Energy and Buildings*, 33(4), 319–331. [https://doi.org/10.1016/S0378-7788\(00\)00114-6](https://doi.org/10.1016/S0378-7788(00)00114-6)
- Dempsey, M. (2006). *Dymola for Multi-Engineering Modelling and Simulation*. I E E E. <https://doi.org/10.1109/VPPC.2006.364294>
- Duffie, J. A., & Beckman, W. A. (1991). *Solar Engineering of Thermal Processes* (Jhon Wiley & Sons Inc., Ed.; 2nd ed.).
- Energy Agency, I. (2021). *Net Zero by 2050 - A Roadmap for the Global Energy Sector*. www.iea.org/t&c/
- Filonenko, K., Copeland, M., Jespersen, K., & Veje, C. (2020). Modeling future heat pump integration in a power radial. *Proceedings of the American Modelica Conference 2020, Boulder, Colorado, USA, March 23-25, 2020*, 169, 130–138. <https://doi.org/10.3384/ecp20169130>
- Grabenweger, P., Lalic, B., Trnka, M., Balek, J., Murer, E., Krammer, C., Možný, M., Gobin, A., Şaylan, L., & Eitzinger, J. (2021). Simulation of daily mean soil temperatures for agricultural land use considering limited input data. *Atmosphere*, 12(4). <https://doi.org/10.3390/atmos12040441>
- Jin, H. (2002). *Parameter estimation based models of water source heat pumps*, Oklahoma State University. <https://hdl.handle.net/11244/46835>
- Jorissen, F., Boydens, W., & Helsens, L. (2018). Validated air handling unit model using indirect evaporative cooling. *Journal of Building Performance Simulation*, 11(1), 48–64. <https://doi.org/10.1080/19401493.2016.1273391>
- Jorissen, F., Reynders, G., Baetens, R., Picard, D., Saelens, D., & Helsens, L. (2018). Implementation and verification of the ideas building energy simulation library. *Journal of Building Performance Simulation*, 11(6), 669–688. <https://doi.org/10.1080/19401493.2018.1428361>
- Kazulis, V., Vigants, H., Veidenbergs, I., & Blumberga, D. (2018). Biomass and natural gas co-firing - Evaluation of GHG emissions. *Energy Procedia*, 147, 558–565. <https://doi.org/10.1016/j.egypro.2018.07.071>
- Koschenz, M., & Lehmann, B. (2000). *Thermoaktive Bauteilsysteme tabs*.
- Luo, X., Wang, J., Dooner, M., & Clarke, J. (2015). Overview of current development in electrical energy storage technologies and the application potential in power system operation. *Applied Energy*, 137, 511–536. <https://doi.org/10.1016/j.apenergy.2014.09.081>
- Olabi, A. G., Onumaegbu, C., Wilberforce, T., Ramadan, M., Abdelkareem, M. A., & Al – Alami, A. H. (2021). Critical review of energy storage systems. *Energy*, 214. <https://doi.org/10.1016/j.energy.2020.118987>
- Olympios, A. V., McTigue, J. D., Farres-Antunez, P., Tafone, A., Romagnoli, A., Li, Y., Ding, Y., Steinmann, W. D., Wang, L., Chen, H., & Markides, C. N. (2020). Progress and prospects of thermo-mechanical energy storage-a critical review. In *Progress in Energy* (Vol. 3, Issue 2). Institute of Physics. <https://doi.org/10.1088/2516-1083/abdbba>
- Vecchi, A., Knobloch, K., Liang, T., Kildahl, H., Sciacovelli, A., Engelbrecht, K., Li, Y., & Ding, Y. (2022). Carnot Battery development: A review on system performance, applications and commercial state-of-the-art. In *Journal of Energy Storage* (Vol. 55). Elsevier Ltd. <https://doi.org/10.1016/j.est.2022.105782>
- Wei, Y., Chen, K., Kang, J., Chen, W., Wang, X., & Zhang, X. (2022). Policy and management of carbon peaking and carbon neutrality: a literature review. *Engineering*, 14, 52–63.
- Wetter, M., & Van Treeck, C. (2017). *New Generation Computational Tools for Building & Community Energy Systems Annex 60*. www.iea-ebc.org

ACKNOWLEDGEMENT

The project source of the results presented in this paper has received funding from the Walloon Region of Belgium, in the frame of the ARDNrgy Project.